ISBN: 978-3-95450-214-1 ISSN: 2673-5490 doi:10.18429/JACoW-IPAC2021-MOPAB027

IMPROVING THE LUMINOSITY BURN-OFF ESTIMATE BY CONSIDERING SINGLE-DIFFRACTIVE EFFECTS

F. F. Van der Veken*, H. Burkhardt, M. Giovannozzi, V. Berglyd Olsen,
CERN Beams Department, Geneva, Switzerland

Abstract

Collisions in a high-luminosity collider result in a continuous burn-off of the circulating beams that is the dominant effect that reduces the instantaneous luminosity over time. In order to obtain a good estimate of the luminosity evolution, it is imperative to have an accurate understanding of the burn-off. Typically, this is calculated based on the inelastic cross-section, as it provides a direct estimate of the number of protons that participate in inelastic collisions, and are hence removed. Likewise, protons that participate in elastic collisions will remain in the machine acceptance, still contributing to luminosity. In between these two regimes lie diffractive collisions, for which the protons have a certain probability to remain in the machine acceptance. Recent developments of the SixTrack code allow it to interface with PYTHIA, thus allowing for more precise simulations to obtain a better estimate of the diffractive part of the cross-section. In this paper, we will mainly concentrate on slowly-drifting protons that are close to the acceptance limit, resulting from single-diffractive scattering.

INTRODUCTION

An accurate estimate of the luminosity $\mathscr{L}$ of a circular collider, and in particular of its time evolution, is paramount to assess, and possibly improve, the expected performance of a particle accelerator. A good understanding of the luminosity could be used e.g. to evaluate the optimal fill duration that maximises the total integrated luminosity [1, 2]. Disregarding the so-called pseudo-diffusive effects (as explained in [1]), the dominant contribution to luminosity evolution is given by the burn-off, i.e. the number of protons that are lost in collisions. For this reason, models to describe the time dependence of luminosity are typically built on the knowledge of the inelastic cross-section, assuming that protons that are scattered elastically remain in the ring acceptance, and might continue contributing to collisions.

However, there are two caveats. First, it does not take diffractive processes into account, which, for the purpose of luminosity, can be considered completely inelastic (this is the case for double-diffractive processes), completely elastic (this is the case for central-diffractive processes), or a combination of both (this is the case for single-diffractive processes). An introduction to these topics and their implementation in PYTHIA can be found in [3]. Second, one needs to carefully assess whether all elastically-scattered protons will indeed contribute to beam collisions with the same probability as the protons in the beam that have not undergone any scattering process from the protons in the other beam. It is therefore not sufficient to simply verify that scattered protons remain in the machine acceptance, as one should investigate how the scattering process alters the transverse beam distribution, considering also that particles in the beam halo contribute much less to the collider's luminosity than those in the core [4]. Finally, one also needs to consider that the validity of the luminosity-evolution model intrinsically depends on the accuracy of the cross-section measurements of the processes under consideration. For instance, the value for the total proton–proton inelastic cross-section at $\sqrt{s} = 13\,\text{TeV}$ obtained by the CMS collaboration [5, 6] is around 13% lower than the values obtained by the TOTEM [7] and ATLAS [8] collaborations. The difference is attributed to low-mass diffractive processes. Note also that for single-diffractive cross-section at $\sqrt{s} = 7\,\text{TeV}$ [9] and $\sqrt{s} = 8\,\text{TeV}$ [10] measurement results are available, however at $\sqrt{s} = 13\,\text{TeV}$ only estimates exist [11, 12]. This is likely to change, as the recent discovery of the odderon [13, 14] has renewed interest in a better understanding of elastic and diffractive hadron processes.

In this paper, we present some preliminary results of the studies carried out to determine when single-diffractive scattered protons remain in the machine acceptance, using a set of operational configurations [15] for the HL-LHC at CERN [16].

BASIC PHYSICS AND KINEMATICS CONSIDERATIONS

The differential cross-section of two-body scattering is characterized by the four-momentum vector Mandelstam-variable t. For small t, the elastic differential cross-section falls exponentially according to

$$\frac{d\sigma}{dt} \propto \exp(-|b|\,|t|) \qquad |t| \approx 2p^2(1-\cos\theta) \approx p^2\theta^2$$

where $|b| \approx 19\,\text{GeV}^{-2}$ for elastic scattering and $|b| \approx 9\,\text{GeV}^{-2}$ for single-diffractive scattering. Based on this, we estimate that 99% of the protons are scattered at $\theta < 76\,\mu\text{rad}$ in case of elastic scattering and with $\theta < 110\,\mu\text{rad}$ in case of single-diffractive scattering. This can be compared to the local angular acceptance of the LHC of roughly 800 µrad, as defined by the TAS absorbers of 17 mm radius at 21 m from the interaction point. Note, however, that this estimate disregards the natural beam divergence of about 47 µrad at 1σ as well as the effect of the crossing angle, which makes the acceptance asymmetric. The typical value of the half crossing angle for the luminosity upgrade of the LHC is 250 µrad, still allowing the single-diffracted protons to remain inside the angular acceptance.

* frederik.van.der.veken@cern.ch

ISBN: 978-3-95450-214-1 ISSN: 2673-5490 doi:10.18429/JACoW-IPAC2021-MOPAB027

Since the protons do not change energy in elastic scattering and the scattering angles remain small, we can safely neglect their contribution to the burn-off lifetime (but there might be some associated emittance growth due to a change in transverse distribution [17, 18]).

For single-diffractive scattering, one of the protons breaks up into secondary particles, that are all lost locally around the interaction region. The other, surviving proton is scattered at small angles largely within the machine acceptance. It will however also change energy, and will be lost when the energy exceeds the momentum acceptance of 3.43×10^{-4} as defined by the RF bucket height [19] .

PYTHIA INTEGRATION IN SIXTRACK

SixTrack is a 6D single-particle symplectic tracking code [20], and is the simulation tool used for this study. SixTrack is modular, and various special elements can be added to the tracking simulations. The "Scatter Module" [21] is one such module, and provides a way to simulate elastic and diffractive scattering processes at, e.g., interaction points. The module has an internal elastic scattering generator, which can be extended by integrating with PYTHIA8 [22,23] to generate single-, double- and central-diffractive events.

When PYTHIA is used as the event generator, SixTrack interfaces with its SoftQCD module in one of two possible ways. The particles from SixTrack can be sent one by one to the PYTHIA library, undergo the chosen scattering processes, for then to be returned for continued tracking. This method takes into account the energy and trajectory of each particle when scattering. A simpler and faster method is to generate scattering events in bulk as head-on collisions at a fixed energy, and then have the deflection and energy loss applied to the particles on the SixTrack side. For this study, the latter method has been used.

NUMERICAL SIMULATIONS

The simulations are performed using the lattice of the luminosity upgrade of the LHC [16], the V1.4 optics, with Landau octupoles off, and using low chromaticity ($Q' = 3$). As far as nonlinear magnetic imperfections are concerned, five different realisations have been used to probe whether nonlinear effects might have an impact on the acceptance for single-diffractive protons. Furthermore, a specific configuration has been investigated that includes nominal octupole strengths and high chromaticity ($Q' = 15$), bringing the total number of machine configurations to six. For all configurations analysed in this study, the collimation system has been included with nominal settings [24, 25].

For each numerical simulation, two initial distributions have been considered: a transverse pencil beam, i.e. a 2D Gaussian distribution in the longitudinal phase space with $\langle \delta^2 \rangle = 1.3 \cdot 10^{-4}$ and $\langle (\Delta s)^2 \rangle = 125\,\text{mm}$ and all transverse coordinates set to zero, and a 6D Gaussian beam in normalised coordinates expressed in beam sigma, with $\langle \hat{x}^2 \rangle, \langle \hat{y}^2 \rangle, \langle \hat{p_x}^2 \rangle, \langle \hat{p_y}^2 \rangle = 1$ for the transverse coordinates and $\langle \hat{z}^2 \rangle = 1.5$ and $\langle \hat{p_z}^2 \rangle = 1.1$ for the longitudinal coordinates (chosen as to adequately fill the bucket area). In both cases, one million particles are randomly sampled and tracked for 100 turns through the lattice. Then, each particle undergoes one single-diffractive scattering event, in which the tracked particle is supposed to be the one that survives, simulated by PYTHIA. Finally, the particles are tracked for 10^4 turns additionally, to assess how the beam distribution evolves. Particle acceptance is defined by two criteria: the scattered particle should not be lost on the ring aperture or on any collimator, and the particle should remain inside the bucket area.

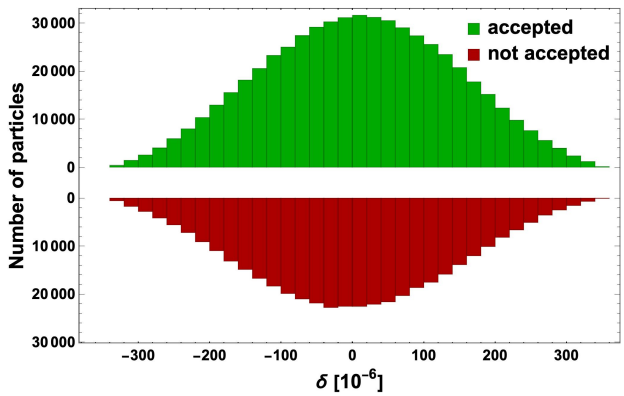

Figure 1: Histogram of the longitudinal distribution of particles, just before scattering, as a function of the relative momentum deviation δ, for one of the machine realisations with Landau octupoles off and with a transverse pencil beam as initial distribution. Upper: particles that remain in the acceptance after scattering. Lower: particles that are no longer in the acceptance after scattering. Shown is the absolute number of particles, such that a visual comparison can be made. It is clear that more than half of the particles remain in the acceptance.

As expected from theoretical considerations, the dominant effect of single-diffractive scattering is a negative kick in δ, the relative momentum offset, hence effectively reducing the particle's energy. A logical conclusion from this is that, at first order, beam acceptance is defined by whether or not the diffractive scattering event kicks the particle out of the bucket area. This is confirmed by our simulations, where all particles that are out of the acceptance after scattering, were those immediately kicked out of the bucket area. Hence, the probability of a particle remaining in the acceptance should be evaluated as a function of δ, only (and possibly the value of the cut introduced by the momentum collimation). An example of this is shown in Fig. 1 for a transverse pencil beam, using one of the machine realisations with Landau octupoles off. It is immediately clear that more than half of the particles remain in the acceptance. Furthermore, we see that the peak of the distribution of accepted particles is slightly shifted towards positive values, while the peak of the distribution of particles that are not accepted is slightly shifted towards negative values: $\langle \delta_{\text{total}} \rangle = 3.40 \cdot 10^{-6}$, $\langle \delta_{\text{accepted}} \rangle = 8.74 \cdot 10^{-6}$, and $\langle \delta_{\text{not accepted}} \rangle = -3.81 \cdot 10^{-6}$.

ISBN: 978-3-95450-214-1 ISSN: 2673-5490 doi:10.18429/JACoW-IPAC2021-MOPAB027

Table 1: Acceptance Expectation

	I_{oct} = 0 A, Q' = 3					I_{oct} = 300 A, Q' = 15
	seed 1	seed 33	seed 38	seed 49	seed 53	seed 1
Transverse Pencil Beam	57.379%	57.142%	57.379%	57.379%	57.379%	57.378%
6D Gaussian	57.292%	57.293%	57.294%	57.295%	57.298%	57.292%

This can intuitively be explained by the fact that particles with lower δ need less of a kick to be out of the bucket area, and hence have a lower probability to remain in the acceptance than particles with higher δ.

We can make this qualitative argument into a quantitative one by binning the data, and calculating for each bin the number of accepted particles as a fraction of the total number of particles in that bin. To get the probability as a smooth function of δ, we repeat this process for different number of bins from 15 up to 200 bins, pairing the centre of the bin with the acceptance fraction explained above. This is shown in Fig. 2, using the same set of particles as in Fig. 1. To obtain the final expectation for the fraction of accepted particles for one specific setup, the binned probability data $P(\delta)$ is fitted and integrated over δ while weighted over the distribution $f(\delta)$ at the moment of scattering:

$$\mathcal{P} = \int \mathrm{d}\delta \; P(\delta) f(\delta) \,. \tag{1}$$

This is repeated for each machine configuration and initial distribution, and the results are reported in Table 1. The results are extremely consistent among the different configurations, with an average probability of around 57% for a particle that is scattered by a single-diffractive process to remain in the acceptance. This implies that the actual machine configuration does not seem to have an impact on the acceptance after the scattering event. Note that this number needs to be divided by two, as in our tracking simulations the particles were always assumed to be the surviving ones, while in reality it has a 50% chance to be destroyed.

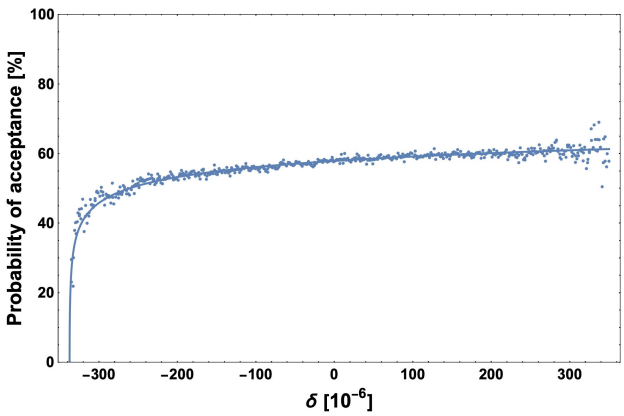

Figure 2: Probability function for a particle to be accepted after single-diffractive scattering, as a function of the relative momentum deviation δ at the moment of scattering. Both the raw data and a fit function are shown.

PRELIMINARY ESTIMATE TO CORRECT LUMINOSITY BURN-OFF

As an example, we can show how our result would influence the estimate of the time evolution of luminosity. The burn-off contribution to the luminosity evolution can be easily shown to equal (see also [1]):

$$L(t) = \frac{\Xi N_i^2}{\left[1 + \sigma_{\mathrm{in}} n_c \, \Xi N_i \, t\right]^2} \,, \tag{2}$$

where N_i is the initial beam intensity (assuming equal beams), σ_{in} is the total inelastic cross-section, Ξ is a scaling factor defined by the machine and its operational settings (see [1]), and n_c is the number of collision points. The caveat is that σ_{in} is typically calculated as the difference between the total cross-section and the elastic cross-section (see e.g. [7]), implicitly assuming that all diffracted protons are destroyed or do not remain in the acceptance. Hence, to account for those protons that remain in the acceptance, we should make the substitution

$$\sigma_{\mathrm{in}} \to \sigma_{\mathrm{in}} - \frac{1}{2} \mathcal{P} \, \sigma_{\mathrm{SD}} \,, \tag{3}$$

where σ_{SD} is the total single-diffractive cross-section and $\mathcal{P}$ is the total probability for a particle to remain in the acceptance as shown in Table 1.

A recent measurement of TOTEM at $\sqrt{s}$ =13 TeV [7] estimated the total and elastic cross-sections at $\sigma_{\mathrm{tot}} = (110.6 \pm 3.4)$ mb and $\sigma_{\mathrm{el}} = (31.0 \pm 1.7)$ mb, giving an estimate of the inelastic cross-section of $\sigma_{\mathrm{in}} = (79.5 \pm 1.8)$ mb. Note that no measurement exists for the single-diffractive cross-section at $\sqrt{s}$ = 13 TeV, though the value is estimated to be at around 12 mb [12]. Our results then imply that, as far as the luminosity evolution is concerned, the value used for the inelastic cross-section should rather be around 76 mb.

CONCLUSIONS AND OUTLOOK

We have shown that, for a limited set of machine configurations of the luminosity upgrade of the LHC, the average expected probability for a proton to remain in the machine acceptance after undergoing a single-diffractive scattering event is around 57%, divided by two to account for the fact that only one out of two protons will survive the collision.

Furthermore, a careful treatment of the errors on the calculated probabilities should be performed, and different models used by PYTHIA to describe diffractive processes should be explored. The results presented in this paper should be considered preliminary, and will be strengthened in a planned follow-up paper, using a wider set of configurations.

ISBN: 978-3-95450-214-1 ISSN: 2673-5490 doi:10.18429/JACoW-IPAC2021-MOPAB027

REFERENCES

[1] M. Giovannozzi and F. F. Van der Veken, "Description of the luminosity evolution for the CERN LHC including dynamic aperture effects. Part I: the model", *Nucl. Instrum. Meth. A*, vol. 905, p. 171-179, 2018. [erratum: *Nucl. Instrum. Meth. A*, vol. 927, p. 471-471, 2019.] doi:10.1016/j.nima.2018.07.063

[2] M. Giovannozzi and F. F. Van der Veken, "Description of the luminosity evolution for the CERN LHC including dynamic aperture effects. Part II: application to Run 1 data", *Nucl. Instrum. Meth. A*, vol. 908, p. 1-9, 2018. doi:10.1016/j.nima.2018.08.019

[3] C. O. Rasmussen and T. Sjöstrand, "Models for total, elastic and diffractive cross sections", *Eur. Phys. J. C*, vol. 78, no.6, p. 461, 2018. doi:10.1140/epjc/s10052-018-5940-8

[4] H. Burkhardt and R. Schmidt, "Intensity and Luminosity after Beam Scraping", CERN, Geneva, Switzerland, Rep. CERN-AB-2004-032-ABP, 2004.

[5] A. M. Sirunyan *et al.*, "Measurement of the inelastic proton-proton cross section at $\sqrt{s}$ = 13 TeV", *JHEP*, vol. 07, p. 161, 2018. doi:10.1007/JHEP07(2018)161

[6] H. Van Haevermaet, "Measurement of the inelastic cross section at $\sqrt{s}$ = 13 TeV", in *Proc. of XXIV International Workshop on Deep-Inelastic Scattering and Related Subjects — PoS(DIS2016)*, 2016, vol.265, p. 198. doi:10.22323/1.265.0198

[7] G. Antchev *et al.*, "First measurement of elastic, inelastic and total cross-section at $\sqrt{s}$ = 13 TeV by TOTEM and overview of cross-section data at LHC energies", *Eur. Phys. J. C*, vol. 79, no. 2, p. 103, 2019. doi:10.1140/epjc/s10052-019-6567-0

[8] M. Aaboud *et al.*, "Measurement of the Inelastic Proton-Proton Cross Section at $\sqrt{s}$ = 13 TeV with the ATLAS Detector at the LHC", *Phys. Rev. Lett.*, vol. 117, no. 18, p. 182002, 2016. doi:10.1103/PhysRevLett.117.182002

[9] V. Khachatryan *et al.*, "Measurement of diffraction dissociation cross sections in pp collisions at $\sqrt{s}$ = 7 TeV", *Phys. Rev. D*, vol. 92, no.1, p. 012003, 2015. doi:10.1103/PhysRevD.92.012003

[10] G. Aad *et al.*, "Measurement of differential cross sections for single diffractive dissociation in $\sqrt{s}$ = 8 TeV pp collisions using the ATLAS ALFA spectrometer", *JHEP*, vol. 02, p. 042, 2020. [erratum: *JHEP*, vol. 10, pp. 182, 2020.] doi:10.1007/JHEP02(2020)042

[11] V. A. Khoze, A. D. Martin, and M. G. Ryskin, "Elastic and diffractive scattering at the LHC", *Phys. Lett. B*, vol. 784, pp. 192-198, 2018. doi:10.1016/j.physletb.2018.07.054

[12] H. Van der Veken, H. Van Haevermaet, and P. Van Mechelen, "Werkzame doorsnede van enkel diffractieve proton-protonbotsingen bij $\sqrt{s}$ = 13 TeV", unpublished Master thesis, University of Antwerp, Belgium.

[13] V. M. Abazov *et al.*, "Comparison of pp and $p\bar{p}$ differential elastic cross sections and observation of the exchange of a colorless C-odd gluonic compound", CERN, Geneva, Switzerland, REP. CERN-EP-2020-236, Dec. 2020. arXiv:2012.03981

[14] T. Csörgő, T. Novak, R. Pasechnik, A. Ster, and I. Szanyi, "Evidence of Odderon-exchange from scaling properties of elastic scattering at TeV energies", *Eur. Phys. J. C*, vol. 81, no. 2, p. 180, 2021. doi:10.1140/epjc/s10052-021-08867-6

[15] G. Arduini *et al.*, "Chapter 2: Machine layout and performance", in *High-Luminosity Large Hadron Collider (HL-LHC): Technical design report*, CERN Yellow Report, 2020, p. 17–46. doi:10.23731/CYRM-2020-0010.17

[16] I. Béjar Alonso, O. Brüning, P. Fessia, L. Rossi, L. Tavian, and M. Zerlauth, *High-Luminosity Large Hadron Collider (HL-LHC): Technical design report*, CERN Yellow Report, Geneva, Switzerland, 2020. doi:10.23731/CYRM-2020-0010

[17] M. Lamont and O. Johnson, "LHC beam and luminosity lifetimes revisited", CERN, Geneva, Switzerland, Rep. CERN-ACC-2014-0255, 2014.

[18] R. Tomás, J. Keintzel, and S. Papadopoulou, "Emittance growth from luminosity burn-off in future hadron colliders", *Phys. Rev. Accel. Beams*, vol. 23, no. 3, p. 031002, 2020. doi:10.1103/PhysRevAccelBeams.23.031002

[19] E. Metral *et al.*, "Update of the HL-LHC operational scenarios for proton operation", CERN, Geneva, Switzerland, Rep. CERN-ACC-NOTE-2018-0002, 2018.

[20] R. De Maria *et al.*, "SixTrack Version 5: Status and New Developments", in *Proc. 10th Int. Particle Accelerator Conf. (IPAC'19)*, Melbourne, Australia, May 2019, pp. 3200–3203. doi:10.18429/JACoW-IPAC2019-WEPTS043

[21] K. N. Sjobak, H. Burkhardt, R. De Maria, and V. K. B. Olsen, "Generalised Scattering Module in SixTrack 5", in *Proc. 10th Int. Particle Accelerator Conf. (IPAC'19)*, Melbourne, Australia, May 2019, pp. 3156–3159. doi:10.18429/JACoW-IPAC2019-WEPTS026

[22] T. Sjostrand, S. Mrenna, and P. Z. Skands, "A Brief Introduction to PYTHIA 8.1", *Comput. Phys. Commun.*, vol. 178, pp. 852-867, 2008. doi:10.1016/j.cpc.2008.01.036

[23] T. Sjostrand, S. Mrenna, and P. Z. Skands, "PYTHIA 6.4 Physics and Manual", *JHEP*, vol. 05, p. 026, 2006. doi:10.1088/1126-6708/2006/05/026

[24] S. Redaelli, R. Bruce, A. Lechner, and A. Mereghetti, "Chapter 5: Collimation system", in *High-Luminosity Large Hadron Collider (HL-LHC): Technical design report*, CERN Yellow Report, 2020, p. 87–114. doi:10.23731/CYRM-2020-0010.87

[25] D. Mirarchi *et al.*, "Cleaning Performance of the Collimation System of the High Luminosity Large Hadron Collider", in *Proc. 7th Int. Particle Accelerator Conf. (IPAC'16)*, Busan, Korea, May 2016, pp. 2494–2497. doi:10.18429/JACoW-IPAC2016-WEPMW030